Deriving information about architecture from activity patterns in coupled cell systems

Krešimir Josić[*]and Jonathan Rubin[†]

April 29, 2004

Abstract

In coupled networks, the properties of the constituent elements (cells), their interactions, and the coupling architecture combine to determine the possible coherent states that may arise. In this work, we examine what can be said about the coupling architecture of a network based on an observed multisynchronous activity pattern, in which cells form multiple synchronized clusters. Specifically, we derive a linear relation, the solutions of which are precisely those coupling architectures that are robustly compatible with a given multisynchronous state. We analyze this relation under the assumption that the network consists of a ring of identical cells, or a ring of two interleaved cell populations. Comparison of these cases shows that coupling of an "observed" layer of cells to a second "hidden" layer can significantly broaden the range of architectures that support certain clustering patterns in the observed cells.

Key words: network coupling architecture, multisynchronous states, balanced coloring

AMS subject classifications: 05C40, 34C14, 34C15, 37C80

Running title: Deriving architecture from activity patterns

1 Introduction

The phenomenon of spontaneous synchronization in networks of coupled systems is ubiquitous in nature, and has been studied in a variety of settings [20, 24]. Many of the theoretical studies of the phenomenon start by postulating models for the individual systems and their interactions in the network. The collective behavior of the network is then analyzed after a particular pattern of connections, or coupling architecture, has been specified. The

[*]Department of Mathematics, University of Houston, Houston, TX 77204-3476

[†]Department of Mathematics and Center for the Neural Basis of Cognition, University of Pittsburgh, Pittsburgh, PA 15260

properties of the individual systems, their interactions, and the coupling architecture are all important in determining the features of the coherent states that appear in such networks.

The present work provides a different approach to the analysis of synchrony in networks. Rather than specifying the properties of the network at the outset, we assume that a particular activity pattern has been observed in the network, but little else is known. The question we begin to address is the following: Can one infer anything about the network's coupling architecture from the fact that it supports the observed mode of activity? More specifically, we ask how a network's capability to produce a particular activity pattern constrains the possible coupling architectures that may be present in the network.

The problem of constructing a network architecture that produces a certain activity pattern has been considered, for instance, to construct networks that can serve as central pattern generators for the various gaits observed in quadrupeds [12, 11]. The approach used in these studies was based on the analysis of the symmetries of the system, which lead to the spatio-temporal patterns of activity corresponding to different gaits. In the present work, we study *multisynchronous* states, featuring multiple synchronized clusters that may be out of synch with each other. Although multisynchronized states may result from the symmetries of a network, such states may not have the full symmetries of the network, and they may also appear in networks that do not possess any symmetries. In general, while it is clear that there is a connection between patterns of synchrony in a network and the network architecture, the relation between the two has, up to this point, been poorly understood.

In contrast to [12, 11], the mathematical methods introduced in this paper rely on local information about architecture and can thus be used to analyze states that do not result from global symmetries of the network. We apply these methods to fully analyze which architectures are compatible with specified multisynchronous states. Examples of synchronous patterns that are not due to symmetry have also been discussed in [10], and we provide a general framework for analyzing the networks that can support such patterns. One direct consequence of this analysis is the result that the presence of a "hidden" layer of cells can strongly impact the range of network architectures that can support a given activity pattern in an "observed" layer of cells.

A significant motivation for studying architectural implications of coherent activity states derives from the field of neuroscience. Experimental and computational evidence suggests that synchronized activity of synaptically interconnected neuronal ensembles contributes to a variety of cognitive tasks, such as attending to regions in the receptive field [9] and recognizing learned spatiotemporal patterns [15, 16]. Moreover, the power of synchronized neuronal oscillations at various frequencies is augmented during certain periods or states, as in cortical gamma rhythms during epochs of attentiveness associated with successful learning [9, 17], thalamic spindle and delta rhythms during periods of sleep [7, 8], and subthalamopallidal oscillations in parkinsonian states (reviewed in [3]). Note that synchronized states relevant to the above examples include states of multisynchrony.

Through biophysically-based computational modeling of neuronal networks, one can attempt to assess the contribution of various features of intrinsic and synaptic dynamics to the occurrence of synchronized states. Computational results also highlight the crucial role that the synaptic architecture, or pattern of synaptic connections between neurons, can play in shaping network behavior (e.g. [25]); indeed, changes in synaptic architecture alone can induce significant changes in firing patterns within a model neuronal network. Unfortunately, experimental information about synaptic architectures, particularly the architecture of effective synapses in a network, is sketchy in many cases. In particular, while it may be possible to ascertain that two general brain areas are synaptically connected (e.g. from viral injection studies [14]), it is much more difficult to establish details about synaptic density, reciprocity, or patterning. Given these difficulties, a theoretical means to infer information about synaptic architecture from the nature of observed activity patterns in a network would represent a valuable tool in computational modeling of neuronal networks. For example, such an inverse approach could be used to constrain the range of synaptic architectures to be considered in simulations and analysis of model network dynamics or to infer information about a biological network based on its experimentally observed activity patterns.

In this work, we take an abstract, model independent approach to the inverse problem of using a network's activity patterns to constrain its coupling architecture. Although we consider only states of exact multisynchrony, the conclusions we obtain are not restricted to any particular type of system. While all patterns of synchrony can be observed in an all-to-all coupled network, we will seek to specify *all* of the architectures that can *robustly* yield given activity patterns. Here, robustness refers to the fact that with these architectures, changes in the intrinsic dynamics of its components will not destroy the specified patterns (as long as the changes are made so that cells in the network which are assumed to be equal remain equal). To focus our investigation, we will assume that cells are arranged in a ring, corresponding to a $\mathbf{Z}_N$ symmetry. Since a ring arises from taking a one-dimensional chain of cells and imposing periodic boundary conditions, rings are the standard architecture assumed in many computational studies of waves, localized activity, and other organized activity patterns in discrete models of neuronal networks. Note, however, that the methods we present will apply in the absence of this symmetry as well.

We emphasize that we consider the mathematical ideal of synchrony: If x_0 and x_1 are the state variables of two systems, then they are synchronous only if $x_0 = x_1$. Implicitly, we will make an even stronger assumption. Given a system of N cells described by internal variables $x_0, \cdots x_{N-1}$, each evolving in state space $\mathbb{R}^m$, two systems x_i and x_j will be able to exhibit synchronous behavior only if the manifold $S_{i,j} = \{(x_0, \cdots, x_{N-1}) \in \mathbb{R}^m : x_i = x_j\}$ contains an invariant submanifold. This is a strong assumption, which may not cover all situations of interest in practice. However, such an assumption is desirable, because if invariant manifolds corresponding to synchronous behavior exist and are stable in an appropriate sense,[1] then the synchronous states persist under small perturbations away from synchrony.

An example of the type of solution we seek is given in Fig. 1. Here, a multisynchronous state is specified by coloring the cells according to their cluster membership, *i.e.* cells sharing the same color are synchronous. Our results yield constraints on the set of all inputs to each cell in the network. When these constraints are satisfied, the input sets for different cells of the same color are equivalent, in the sense that, for each color appearing in the network,

[1] In fact normal hyperbolicity is necessary and sufficient.

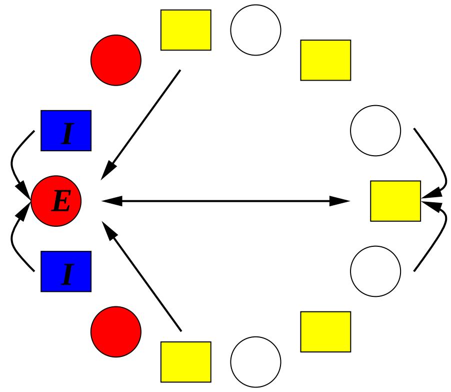

Figure 1: An example of a balanced coloring with E cell clusters of sizes 3 and 4, and I cell clusters of sizes 2 and 5, achieved within a double ring. The connection pattern shown repeats for all cells in the network, such that each red E cell receives inputs from 2 blue I cells and 3 yellow I cells; each white E cell receives inputs from 1 blue I cell and 4 yellow I cells; each blue I cell receives inputs from 2 red E cells and 1 white E cells; and each yellow I cell receives inputs from 1 red E cell and 2 white E cells.

the input sets contain the same number of elements of that color. Fig. 1 illustrates an architecture that achieves this balance, although it is not the only such architecture. We will show that, without assuming the existence of a layer of I cells (the rectangular cells in the figure), only a network with all-to-all coupling can support the 2-cluster multisynchronous pattern in the E cells shown in Fig. 1. Therefore, the existence of a "hidden" layer of cells allows for a much sparser network architecture, as seen in Fig. 1.

In the next section, we give a more thorough introduction of the notation and terminology, such as the notions of an inputs set and a balanced coloring, that are useful for our approach. Further, we derive the general mathematical formulation of the architectural specification problem that we will consider. In Section 3, we state and prove our first main result, on architectures that support two-cluster solutions on a ring. We also present an example of the application of our result to a particular solution and ring, and we discuss general ways to check the connectedness of architectures. In Section 4, we state and prove our second main result, on multisynchronous solutions in rings of two interleaved cell types, providing an example of how the presence of a second cell type can weaken strict architectural constraints that would be required for certain activity patterns to arise in a ring of just one cell type. We conclude with a discussion in Section 5.

2 Notation and mathematical description of the problem

The main idea of our approach is to translate the problem of constructing an architecture that allows for certain patterns of multisynchrony into the problem of finding integer solutions to a set of linear equations. In this section, we introduce notation and illustrate our approach in a simple example.

2.1 Multisynchrony in a small example network

For simplicity, we first consider networks of identical cells, so that each cell evolves in the same phase space as the others. The *connectivity matrix* A of the network is a matrix of non-negative integers, where an entry $a_{i,j}$ denotes the number of connections *from cell* j *to cell* i. We assume that the connections between the cells in the network are identical to avoid introducing multiple connectivity matrices. Fig. 2 provides an example of a six cell network and its connectivity matrix.

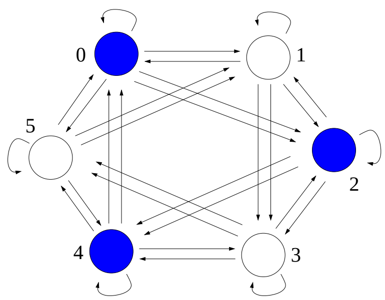

$$A = \begin{bmatrix} 1 & 1 & 0 & 0 & 2 & 1 \\ 1 & 1 & 1 & 0 & 0 & 2 \\ 2 & 1 & 1 & 1 & 0 & 0 \\ 0 & 2 & 1 & 1 & 1 & 0 \\ 0 & 0 & 2 & 1 & 1 & 1 \\ 1 & 0 & 0 & 2 & 1 & 1 \end{bmatrix}$$

Figure 2: An example of a network of six identical cells and its connectivity matrix.

The structure of a network has to be reflected in the equations that are used to model it. In particular, if the internal states of the cells in the network of Figure 2 are denoted by $x_i \in \mathbf{R}^k$ for $i = 0, \ldots, 5$, and we set $x = (x_0, x_1, x_2, x_3, x_4, x_5)$, then a differential equation modeling the evolution of this network must have the form

$$\begin{aligned} x_0' &= f(x_0, x_1, x_4, x_4, x_5) & \qquad x_3' &= f(x_3, x_4, x_1, x_1, x_2) \\ x_1' &= f(x_1, x_2, x_5, x_5, x_0) & \qquad x_4' &= f(x_4, x_5, x_2, x_2, x_3) \\ x_2' &= f(x_2, x_3, x_0, x_0, x_1) & \qquad x_5' &= f(x_5, x_0, x_3, x_3, x_4) \end{aligned} \tag{2.1}$$

It can be checked by direct substitution that the linear submanifolds $Y_1 = \{x : x_i = x_j \text{ for all } i \text{ and } j\}$ and $Y_2 = \{x : x_0 = x_2 = x_4 \text{ and } x_1 = x_3 = x_5\}$ are invariant under the evolution of system (2.1), *i.e.* solutions with initial conditions in Y_1 and Y_2 remain in Y_1 and Y_2, respectively, for all time. Therefore, any differential equation model of the network given in Fig. 2 supports both the fully synchronous state $x = (x(t), x(t), x(t), x(t), x(t), x(t))$ and the multisynchronous state $x = (x_0(t), x_1(t), x_0(t), x_1(t), x_0(t), x_1(t))$.

We note that the *existence* of these states is a consequence only of the assumed network architecture (in this case, the $\mathbf{Z}_N$ symmetry of the network). Other features, such as the stability of the synchronous states, depend on the details of the model's dynamics.

2.2 Multisynchronous states in general networks

It is natural to ask what multisynchronous states a given network architecture can support. This problem has been explored in detail in [23, 13]. Our present goal is to provide a general approach to answering the inverse question: Given a particular multisynchronous state, what are the network architectures that can support it? In this section we introduce the notation we use to describe a general multisynchronous state and the conditions on the network architecture that allow the network to support such states.

To describe a pattern of multisynchrony in a network of N cells, we first number the cells in the network. Each cell is then assigned a vector $c_i \in \mathbf{R}^m$, where m is the number of synchronous clusters that appear in the multisynchronous solution of interest. Each c_i will be a unit vector from the standard basis $\{e_1, \ldots, e_m\}$ for $\mathbf{R}^m$, and the position of the nonzero element of the vector will denote which group of synchronous cells the cell i belongs to. Therefore, cell i is synchronous with cell j if and only if $c_i = c_j = e_l$ for some $l \in \{1, \ldots, m\}$.

Let $\mathcal{C}_i = \{i_0, \ldots, i_{k-1}\}$ and $\mathcal{C}_j = \{j_0, \ldots, j_{l-1}\}$ be the collections of cells that provide inputs to cells i and j, respectively, or their *input sets*. If a single cell provides n inputs to cell i, it is listed n times in $\mathcal{C}_i$. It is shown in [23, 13] that two cells in a network can be expected to be synchronous, in general, only if their input sets are identical. More precisely, the cells i and j can in general be expected to be synchronous only if there exists a bijection $\phi : \mathcal{C}_i \to \mathcal{C}_j$ such that if $\phi(i_r) = j_q$, then $c_{i_r} = c_{j_q}$; under this condition, ϕ maps input cells from any fixed synchronous group to input cells from the same synchronous group.

This observation can be translated into an equation by using the notation established above. Let $\sum_{k=0}^{N-1} a_{i,k} c_k = R_i$, so that R_i is the m-vector whose l-th entry is equal to the number of inputs cell i receives from the synchronous cluster l. The requirement that the cells i and j have the same input set is equivalent to the requirement that

$$\sum_{k=0}^{N-1} a_{i,k} c_k = R_i = R_j = \sum_{k=0}^{N-1} a_{j,k} c_k. \tag{2.2}$$

Following [23, 13], we refer to a fixed assignment of cells into clusters as a *coloring* of the network. For a given coloring and coupling architecture, if (2.2) holds for all i, j such that $c_i = c_j$, then we say that the coloring is *balanced.* Notice that such multisynchronous states are *robust* in the sense that they persist under perturbations which preserve the network architecture, as stated in the following result.

Theorem 2.1 ([23, 13]) *A coloring is balanced if and only if the corresponding multisynchronous state is robust.*

Now, set $c = [c_1, \cdots, c_N]^T \in \mathbf{R}^{mN}$, representing a pattern of synchrony. Using equation (2.2), the problem of finding an architecture such that the coloring associated with the specified multisynchronous m-cluster state is balanced becomes the problem of finding a connectivity matrix $A \in \mathbf{R}^{N \times N}$ and a vector $R = [R_1, \ldots, R_N]^T \in \mathbf{R}^{mN}$, both with non-negative integer entries, such that

$$(A \otimes I_m) c = R. \tag{2.3}$$

In (2.3), I_m is the m by m identity matrix and $\otimes$ denotes the tensor product.

A more geometric interpretation of this condition is the following: Let $\mathcal{R}_c$ be the linear subspace of $\mathbf{R}^{mN}$ defined by $\mathcal{R}_c = \{R = (R_1, R_2, \dots R_N) \in \mathbf{R}^{mN} : R_i = R_j$ whenever $c_i = c_j\}$. Equation (2.3) implies that the problem of finding a network architecture that supports a given pattern of synchrony c is equivalent to finding a matrix A that maps the given pattern of symmetry c to a point in $\mathcal{R}_c$ with non-negative integer components. Note that $\mathcal{R}_c$ has dimension m^2 since each of the m synchronous clusters is characterized by a corresponding m-vector. Note further that it does not matter *which* point in $\mathcal{R}_c$ is attained; the important point is to find an A such that $(A \otimes I_m)c$ is in $\mathcal{R}_c$.

Example: Consider a *ring* of four cells, denoted by $c_0, \dots, c_3$. Suppose that we want to find an architecture that supports two synchronized clusters, in which cells 0 and 1 share one color and cells 2 and 3 share another color. Following the notation above, we set

$$c_0 = c_1 = \begin{bmatrix} 1 \\ 0 \end{bmatrix} \text{ and } c_2 = c_3 = \begin{bmatrix} 0 \\ 1 \end{bmatrix}.$$

Our assumption that we are dealing with a ring of cells means that the network has $\mathbf{Z}_4$ symmetry when the coloring is not taken into account (see Fig. 3). As a consequence, the matrix A is circulant, so that

$$A = \begin{bmatrix} a_0 & a_1 & a_2 & a_3 \\ a_3 & a_0 & a_1 & a_2 \\ a_2 & a_3 & a_0 & a_1 \\ a_1 & a_2 & a_3 & a_0 \end{bmatrix}.$$

The condition that the coloring is balanced is equivalent to requiring that the following equations can be satisfied by some nonnegative integers a_0, a_1, a_2, a_3 and 2-vectors of nonnegative integers R and S

$$\begin{aligned} a_0c_0 + a_1c_1 + a_2c_2 + a_3c_3 &= R & \qquad a_2c_0 + a_3c_1 + a_0c_2 + a_1c_3 &= S \\ a_3c_0 + a_0c_1 + a_1c_2 + a_2c_3 &= R & \qquad a_1c_0 + a_2c_1 + a_3c_2 + a_0c_3 &= S \end{aligned} \tag{2.4}$$

Through a simple manipulation of (2.4) we obtain the following system of equations

$$\begin{aligned} a_0 + a_1 &= R_0 & \qquad a_2 + a_3 &= R_1 \\ a_3 + a_0 &= R_0 & \qquad a_1 + a_2 &= R_1, \end{aligned} \tag{2.5}$$

and four more redundant equations. These equations imply $a_1 = a_3$, while a_0 and a_2 are arbitrary. R and S are determined once the values of $a_0, a_1 = a_3$, and a_2 are set. a_0 describes the coupling of a cell to itself, and can be thought of as one of a cell's intrinsic characteristics.

The three possibilities with single arrows between cells, and $a_0 = 0$, are shown in Fig. 3. Note that when $a_1 = a_2 = a_3 = 1$ we have all-to-all coupling. Since any coloring will be balanced for such a coupling, this solution is uninteresting. Moreover, when $a_1 = a_3 = 0$ and $a_2 = 1$ (Fig. 3C), the network consists of two disconnected subnetworks. We also consider such solutions uninteresting. Therefore the only nontrivial solution in this example is given by $a_1 = a_3 = 1$, and $a_2 = 0$, as in Fig. 3B.

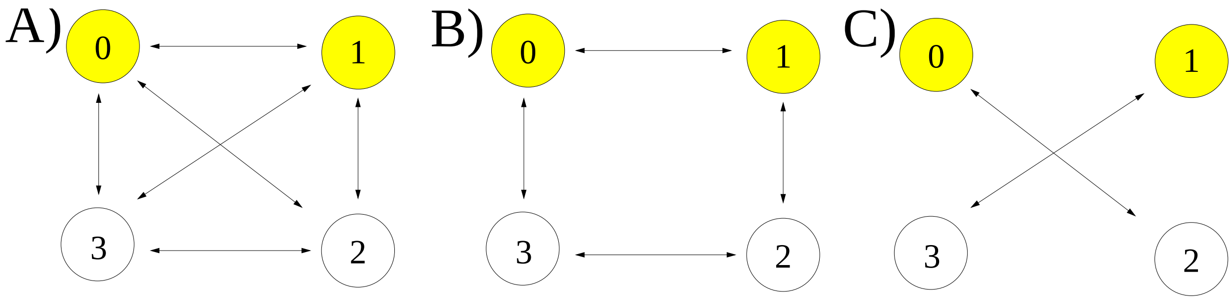

Figure 3: Three possible architectures with single arrows leading to a balanced coloring in a ring with the synchrony pattern described in the text. From left to right A) $a_1 = a_2 = a_3 = 1$, B) $a_1 = a_3 = 1, a_2 = 0$, C) $a_1 = a_3 = 0, a_2 = 1$. In all cases $a_0 = 0$, corresponding to no self-coupling.

Remark 2.2 *To keep the exposition concise, we do not deal with networks in which all cells and connections are not identical, such as neuronal networks with multiple forms of neurotransmitters and receptors. The precise relation between the network architecture and the structure of the system of equations that models the network, as well as the machinery necessary to analyze this relation, is introduced in [23, 13].*

The reader may have noticed that the connectivity matrices for the networks given in Fig. 3B and 3C sum to give the connectivity matrix of the network in Fig.3A. This is a consequence of the following general result

Proposition 2.3 *The set of matrices* $\mathcal{A}_c = \{A \in \mathbf{Z}^{N\times N} : A$ *satisfies (2.3) for some* $R \in \mathcal{R}_c\}$ *forms a module over the integers.*

Proof: Suppose that A and B satisfy (2.3) for $R^A \in \mathcal{R}_c$ and $R^B \in \mathcal{R}_c$, respectively, and a fixed c. If cells i and j are synchronous, then

$$\sum_{k=0}^{N-1} a_{i,k} c_k = R_i^A = R_j^A = \sum_{k=0}^{N-1} a_{j,k} c_k \tag{2.6}$$

and similarly for B and R^B. Therefore $kA+lB$ satisfies (2.3) with the input vector kR^A+lR^B. Since $\mathcal{R}_c$ is a linear subspace, it contains $kR^A + lR^B$. □

Remark 2.4 *The subset of the module* $\mathcal{A}_c$ *consisting of matrices with non-negative entries is the set of all connectivity matrices that satisfy (2.3) for some* $R \in \mathcal{R}_c$.

Note that matrix $\mathbf{O}$ with all entries equal to 1, *i.e.* $[\mathbf{O}]_{i,j} = 1$ for all i, j, is in $\mathcal{A}_c$ for any c. Therefore any multisynchronous solution is supported in an all-to-all coupled network. Suppose that $A \in \mathcal{A}_c$ represents a network with at most single connections between cells. Then $\bar{A} = \mathbf{O} - A$ is in $\mathcal{A}_c$, and represents another network with at most single connections between cells. We call $\bar{A}$ the *complement* of A, and refer to the two networks whose connectivities are given by matrices A and $\bar{A}$ as *complementary networks*. In particular, the networks given in Fig. 3B and 3C are complementary networks.

2.3 Restrictions on architecture

With no restrictions on the matrix A, the problem of solving (2.3) for a given pattern of synchrony c is not interesting. Both an all-to-all coupled network, and a network in which all cells are only coupled with themselves, support all patterns of synchrony, and the problem becomes trivial in these cases.

Another type of trivial solution is provided by a disconnected network. Consider the network shown in Fig. 4. This 9-cell network supports a multisynchronous solution with clusters of 3 and 6 cells. Upon closer inspection (Fig. 4B), one can see that this network is really a union of 3 equal networks of 3 cells. We consider such solutions trivial, since there are no interactions between the cells in the separate networks, and therefore the synchronous states cannot be stable.

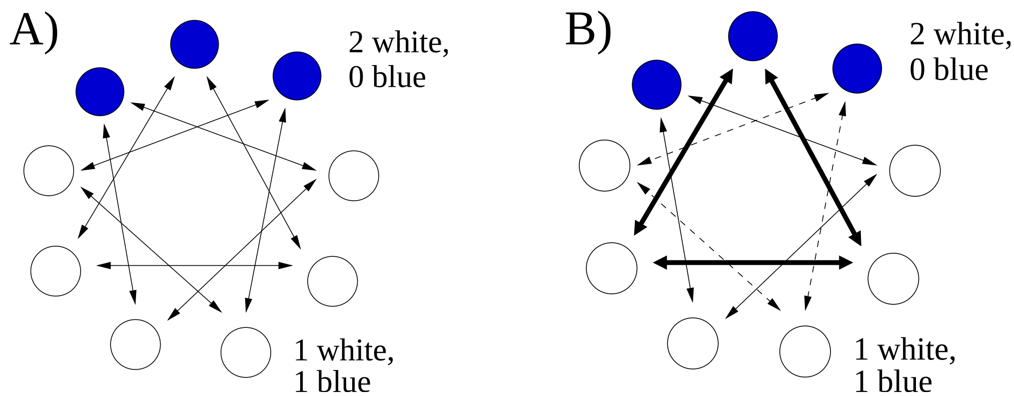

Figure 4: A balanced coloring for a 2-cluster solution in a network of nine cells. The text in this and subsequent figures indicates the numbers of connections to each cell of each type. On the right, we have used three different arrow types to emphasize that this architecture consists of three disconnected components.

In contrast to these trivial architectures, naturally occurring networks are frequently observed or assumed to have a certain non-trivial but patterned structure, which is reflected in the coupled cell systems used to model them. If we assume certain reasonable restrictions on the structure of the networks under consideration, the problem of constructing an architecture that supports a given pattern of synchrony becomes more interesting and informative. As discussed in the introduction, ring architectures are ubiquitous in models of neuronal networks, as well as models of other systems. Therefore, in the following, as in the example above, we consider networks of cells with $\mathbf{Z}_N$ symmetry.

The approach we describe here can be directly extended beyond this case. It is important, however, to specify a class of architectures at the outset, to avoid an overabundance of solutions. A restriction on architecture can be given by imposing a certain symmetry of the architecture, as we have done, or it could be made more general [23, 13]. The constraint used here translates into a constraint on the connectivity matrix A. With this constraint, the problem consists of finding solutions of (2.2) within the specified class of connectivity matrices given a particular multisynchronous pattern.

In Section 3, we will consider 2-cluster multisynchronous solutions in rings of one cell type. The ideas derived there generalize to networks composed of cells of different types. In particular, in Section 4, we consider multi-cluster solutions in rings consisting of two different cell populations that alternate positions around each ring. In the neuronal context, interactions of cells of two distinct types are of particular interest because local neuronal circuits *in vivo* commonly consist of interacting excitatory (E) and inhibitory (I) populations, such as thalamocortical relay (E) and thalamic reticular (I) cells in the thalamus; the subthalamic nucleus (E) and the globus pallidus (I) in the basal ganglia; and pyramidal cells (E) and interneurons (I) in most cortical areas. Note that the theory we develop allows for different types of connections, such as excitatory and inhibitory, between cells, as long as connections emanating from all cells within a single cluster are of the same type.

One interesting result that arises from our approach is that, in some cases where rings of identical cells can only support patterns of synchrony if the network is equipped with a trivial (uncoupled or all-to-all coupled) architecture, the presence of two types of cells (such as the E and I cells discussed above) can greatly broaden the range of architectures that support multisynchronous states.

Example: Consider a ring of 7 E cells shown in Fig. 1. It follows from Corollary 3.3, proved in the next section, that solutions with synchronous clusters of 2 and 5 cells, or of 3 and 4 cells, require all-to-all coupling.

Suppose that we instead consider a ring consisting of alternating E and I cells. While the dynamics of the I cells may or may not be of interest in their own right, we shall see that it is important to take their presence into account when analyzing E cell activity.

In a network of 7 E cells alternating with 7 I cells, it is possible to produce a nontrivial balanced coloring of four colors with clusters of sizes 3, 4 (E cell clusters), 2, and 5 (I cell clusters); see Figure 1 for an example. This balance is achieved by an architecture in which each E cell sends connections to its nearest neighbors (which are I cells) and to the I cell directly across the ring from itself, while each I cell sends connections to its nearest neighbors (which are E cells), to its next-nearest neighbor E cells, and to the E cell directly across the ring. This result does not require any E-E or I-I connections but will be preserved under the inclusion of all-to-all E-E and/or I-I connections, based on Corollary 3.3.

Thus, the presence of a “hidden” layer of cells can allow for particular multisynchronous solutions to emerge in an “observed” layer of cells, even though it would not be possible to obtain these same patterns with a nontrivial architecture in a ring of just a single cell type. We emphasize that, although there are no E-E or I-I connections, this architecture is nontrivial due to the connections between the cells of different type. Although the E cells do not interact directly in such a network, their activity is shaped by their indirect interactions through the I cells.

3 Rings of cells with two synchronous clusters

In this section we assume that the architecture of a network of N identical cells has $\mathbf{Z}_N$ symmetry, so that the cells form a ring. We assume that two groups of adjacent cells form synchronous clusters and we answer the question: What architectures support the given pattern of synchrony?

The assumption of $\mathbf{Z}_N$ symmetry implies that the connectivity matrix A is circulant. We could refer to the well studied properties of circulant matrices to slightly shorten the discussion that follows [6]. In fact, using the particular structure of the equations, a trick can be used to solve them directly, as will be shown in the proof of Theorem 4.1. However, we take a more general approach because the ideas used will also apply whenever the network is assumed to be Γ symmetric[2], for an abelian group Γ. In this situation the irreducible representations of Γ can be used to diagonalize the connectivity matrix A in the way illustrated below.

3.1 Setup and Main Result

Consider a ring of N cells that is separated into two groups of adjacent cells of sizes k and $N-k$. The k cells in the first group are numbered 0 through $k-1$, while cells in the second group are numbered k through $N-1$. Following the notation introduced in section 2.2, we have $c_0 = \ldots = c_{k-1} = \begin{bmatrix} 1 \\ 0 \end{bmatrix}$ and $c_k = \ldots = c_{N-1} = \begin{bmatrix} 0 \\ 1 \end{bmatrix}$.

As shown in section 2.2, the problem of finding an architecture that supports this pattern of synchrony reduces to finding a connectivity matrix A that satisfies equation (2.3) with $m = 2$. Under the assumption that the cells form a ring, equation (2.3) has the form

$$\begin{array}{ll}
a_0 + a_1 + \ldots + a_{k-1} = R_0 & a_k + a_{k+1} + \ldots + a_{N-1} = R_1 \\
a_{N-1} + a_0 + \ldots + a_{k-2} = R_0 & a_{k-1} + a_k + \ldots + a_{N-2} = R_1 \\
\ldots & \ldots \\
a_{N-k+1} + a_{N-k+2} + \ldots + a_0 = R_0 & a_1 + a_2 + \ldots + a_{N-k} = R_1 \\
a_{N-k} + a_{N-k+1} + \ldots + a_{N-1} = S_0 & a_0 + a_1 + \ldots + a_{N-k-1} = S_1 \\
a_{N-k-1} + a_{N-k} + \ldots + a_{N-2} = S_0 & a_N + a_0 + \ldots + a_{N-k-2} = S_1 \\
\ldots & \ldots \\
a_1 + a_2 + \ldots + a_k = S_0 & a_{k+1} + a_{k+2} + \ldots + a_0 = S_1
\end{array} \tag{3.7}$$

It is straightforward to check, by subtracting successive equations, that the equations in the left and right columns of (3.7) are equivalent. We will therefore only deal with the equations in the left column. To simplify computations, we reorder these equations, putting the first equation first, and then following with the last equation up to the second equation, although this step is not essential.

[2]We hope that similar ideas are also applicable when "symmetries" of the system are given by a groupoid, rather than a group [23]. Unfortunately, a representation theory of groupoids that would be applicable to such examples does not seem to have been developed yet.

Once reordered, these equations can be written as

$$Ma = R \tag{3.8}$$

where $a = (a_0, a_1, \ldots, a_{N-1})^T$ and $R = (R_0, \underbrace{S_0, \ldots, S_0}_{N-k\text{times}}, R_0, \ldots, R_0)^T$. Here

$$M = \begin{bmatrix} 1 & 1 & 1 & \ldots & 1 & 0 & 0 & \ldots & 0 & 0 \\ 0 & 1 & 1 & \ldots & 1 & 1 & 0 & \ldots & 0 & 0 \\ 0 & 0 & 1 & \ldots & 1 & 1 & 1 & \ldots & 0 & 0 \\ & & & \ldots & & & & \ldots & & \\ 1 & 1 & 1 & \ldots & 0 & 0 & 0 & \ldots & 0 & 1 \end{bmatrix} \tag{3.9}$$

where each row contains $N - k$ zero entries.

Since we are not fixing the value of R (rather, it is determined after the coefficients in a are set), the problem of interest is equivalent to finding all vectors of positive integers a such that

$$Ma \in V \tag{3.10}$$

where

$$V = R_0 w_1 \oplus S_0 w_2 \stackrel{\text{def}}{=} R_0(1, 1, 1, \ldots, 1)^T \oplus S_0(1, 0, 0, \ldots, 0, 1, 1, \ldots, 1)^T.$$

This problem is solved in the proof of the following theorem. Note that henceforth, we use the notation $M =$ circ $(m_0, m_1, \ldots, m_{N-1})$ to denote a circulant matrix with first row $(m_0, m_1, \ldots, m_{N-1})$.

Theorem 3.1 *Suppose that a network of N cells has $\mathbf{Z}_N$ symmetry. The only architectures that support two synchronous clusters of adjacent cells of sizes k and $N - k$ are described by coupling matrices of the form*

$$A = \text{ circ } (\beta_0, \alpha_1, \ldots, \alpha_{G-1}, \alpha_0, \alpha_1, \ldots \alpha_{G-1}, \alpha_0, \ldots, \ldots, \alpha_{G-1}), \tag{3.11}$$

where $\beta_0, \alpha_0, \ldots \alpha_{G-1} \in \mathbf{N} \cup \{0\}$, and $G = gcd(k, N)$.

Proof: If Γ is an abelian group, and M commutes with Γ, then M can be diagonalized using the irreducible subspaces associated with the action of Γ as a basis. When $\Gamma = \mathbf{Z}_N$, these subspaces can be computed directly, and are given in complex coordinates as $V_i = \mathbf{C}(1, \xi^i, \xi^{2i}, \ldots, \xi^{(N-1)i})$, where $\xi = \exp(2\pi i/N)$ is the N-th root of unity and $\mathbf{C}$ is the field of complex numbers. We can therefore diagonalize M to obtain $\tilde{M} = C^{-1}MC$ where

$$C = \begin{bmatrix} 1 & 1 & 1 & \ldots & 1 \\ 1 & \xi & \xi^2 & \ldots & \xi^{N-1} \\ 1 & \xi^2 & \xi^4 & \ldots & \xi^{2(N-1)} \\ & & \ldots & & \\ 1 & \xi^{N-1} & \xi^{2(N-1)} & \ldots & \xi^{(N-1)^2} \end{bmatrix}.$$

It is straightforward to compute

$$C^{-1} = \frac{1}{N} \begin{bmatrix} 1 & 1 & 1 & \dots & 1 \\ 1 & \xi^{-1} & \xi^{-2} & \dots & \xi^{-(N-1)} \\ 1 & \xi^{-2} & \xi^{-4} & \dots & \xi^{-2(N-1)} \\ & & \dots & & \\ 1 & \xi^{-(N-1)} & \xi^{-2(N-1)} & \dots & \xi^{-(N-1)^2} \end{bmatrix}.$$

Note that our original problem (3.10) is equivalent to

$$[C^{-1}MC]C^{-1}a = \tilde{M}C^{-1}a \in C^{-1}V, \tag{3.12}$$

where the fact that $\tilde{M}$ is diagonal will simplify subsequent calculations. Direct computation gives

$$C^{-1}MC = \tilde{M} = \text{ diag } \left(\sum_{i=0}^{N-1} m_i, \sum_{i=0}^{N-1} m_i \xi^i, \sum_{i=0}^{N-1} m_i \xi^{2i}, \dots, \sum_{i=0}^{N-1} m_i \xi^{(N-1)i} \right)$$

In particular, if the circulant matrix in our example has the form $M = \text{ circ } (m_0, m_1, \dots, m_{N-1}) = \text{ circ } (1, 1, \dots, 1, 0, 0, \dots, 0)$ where the first k entries are 1's, then we have

$$\begin{aligned} \tilde{M} &= \text{ diag } \left(\sum_{i=0}^{k-1} m_i, \sum_{i=0}^{k-1} m_i \xi^i, \sum_{i=0}^{k-1} m_i \xi^{2i}, \dots, \sum_{i=0}^{k-1} m_i \xi^{(N-1)i} \right) && (3.13) \\ &= \text{ diag } (\lambda_0, \lambda_1, \dots, \lambda_{N-1}) && (3.14) \end{aligned}$$

The following proposition is easy to check from this form.

Proposition 3.2 *The matrix M has zero eigenvalues only when $G = gcd(k, N) \neq 1$. If this condition holds, then*

$$\lambda_{\frac{lN}{G}} = \sum_{i=0}^{k-1} \xi^{\frac{lNi}{G}} = 0 \qquad \textit{for } l = 1,\ 2,\ \dots, G-1.$$

Proof: Only when the conditions of the proposition is satisfied, the k complex roots ξ^{mi} are equidistributed around the unit circle, so that their center of gravity is 0. □

It follows from this proposition that the kernel of M has dimension $G - 1$. Therefore $M^{-1}V$, where the inverse is meant in a set theoretic sense, has dimension at most dim(ker M) + dim(V) $= G + 1$.

Next we compute a. Specifically, we use $\tilde{M}C^{-1}a \in C^{-1}V$, and our goal is to find the vectors of natural numbers a that satisfy this relation. It will be easiest to work in $\mathbf{C}^N$ to obtain the linear space $C\tilde{M}C^{-1}V = M^{-1}V$, and complete the problem by finding the intersection of this space with the lattice of natural numbers.

Since V is a linear subspace, it is sufficient to proceed in two steps. We start by finding the kernel of $\tilde{M}$ and the inverse of $R_0 w_1$, after which we compute the inverse of $S_0 w_2$.

Let e_i be the i-th unit vector. Since $\tilde{M}$ is diagonal, a direct computation shows that

$$\tilde{M}^{-1}C^{-1}(\mathbf{C}w_1) = \mathbf{C}e_0 \oplus \bigoplus_{i=1}^{G-1} \mathbf{C}e_{\frac{iN}{G}}. \tag{3.15}$$

The right hand side of equation (3.15) is written as a sum, since $\mathbf{C}e_0$ is a vector space that is not in the kernel, and gets mapped onto $\mathbf{C}w_1$, while the remainder, $\bigoplus_{i=1}^{G-1} \mathbf{C}e_{\frac{iN}{G}}$, comes from the kernel of $\tilde{M}$.

We next need to find the image of the subspace in (3.15) under C to determine the space that the coefficients in a can come from. A direct computation gives

$$C\tilde{M}^{-1}C^{-1}(\mathbf{C}w_1) = \{ \left(\sum_{i=0}^{G-1} c_i \xi^0, \sum_{i=0}^{G-1} c_i \xi^{\frac{iN}{G}}, \sum_{i=0}^{G-1} c_i \xi^{\frac{2iN}{G}}, \ldots, \sum_{i=0}^{G-1} c_i \xi^{\frac{miN}{G}}, \ldots \right)^T, \quad \text{where } c_0, \ldots c_{G-1} \in \mathbf{C}\} \tag{3.16}$$

It can be checked directly that in the vector defined on the right hand side of (3.16), every G-th entry is the same. This divides the vector into G equivalence classes. In particular, the following is true.

$$C\tilde{M}^{-1}C^{-1}(\mathbf{C}w_1) \cap \mathbb{N}^N = \{(\alpha_0, \alpha_1, \ldots, \alpha_{G-1}, \alpha_0, \alpha_1, \ldots \alpha_{G-1}, \alpha_0, \ldots, \ldots, \alpha_{G-1})^T, \quad \text{where } \alpha_0, \ldots \alpha_{G-1} \in \mathbb{N}\}.$$

For the second step, a similar argument can be used to obtain $C\tilde{M}^{-1}C^{-1}(\mathbf{C}w_2)$, but it is sufficient to notice that $M(\mathbf{C}e_0) = \mathbf{C}w_2$, so that the space that we are missing is just $\mathbf{C}e_0$, where $e_0 = (1, 0, 0, \ldots 0)^T$.

This completes the computation, and shows that

$$M^{-1}V \cap \mathbb{N}^N = \{(\beta_0, \alpha_1, \ldots, \alpha_{G-1}, \alpha_0, \alpha_1, \ldots \alpha_{G-1}, \alpha_0, \ldots, \ldots, \alpha_{G-1})^T, \text{ where } \beta_0, \alpha_0, \ldots \alpha_{G-1} \in \mathbb{N}\}.$$

□

Since we do not allow architectures in which the only coupling is self-coupling, two simple corollaries follow from this result; the second is a special case of the first.

Corollary 3.3 *If $gcd(k, N) = 1$, then a balanced coloring requires all-to-all coupling.*

Corollary 3.4 *In a ring of coupled, identical cells, the only way to balance a coloring in which one cell is of one color and all other cells are of a second color is an all-to-all coupling scheme, with possible self-coupling.*

Remark 3.5 *In the proof of Theorem 3.1, $M^{-1}V$ is computed indirectly by looking at $C\tilde{M}^{-1}C^{-1}V$. As noted in the introduction to this section, and illustrated in the proof of Theorem 4.1, it is possible to find $M^{-1}V$ directly using the $\mathbf{Z}_N$ structure. In the case of a general abelian group Γ no such tricks are available, and some computation is needed to find the kernel of M. Finding the kernel is much simpler once this matrix is block diagonalized using the irreducible representations of Γ, as was done in the proof of Theorem 3.1.*

3.2 An example and remarks on $\mathbf{D}_N$ symmetry

In general, the network architectures we obtain have symmetries that form a subgroup of $\mathbf{Z}_N$. Rings of cells that are used as models of neuronal networks frequently have reflectional symmetry, in addition to $\mathbf{Z}_N$ symmetry. Such networks are $\mathbf{D}_N$ symmetric, and the following is an immediate corollary of the results discussed in the previous section.

Corollary 3.6 *Suppose that a network of N cells has $\mathbf{D}_N$ symmetry. The only architectures that support two synchronous clusters of adjacent cells of sizes k and $N-k$ are described by the coupling matrix*

$$A = \; circ\,(\beta_0, \alpha_1, \ldots, \alpha_{G-1}, \alpha_0, \alpha_1, \ldots \alpha_{G-1}, \alpha_0, \ldots, \ldots, \alpha_{G-1}),$$

where $\beta_0, \alpha_0, \ldots \alpha_{G-1} \in \mathbf{N} \cup \{0\}$, $G = gcd(k, N)$, and

$$\alpha_{G-j} = \alpha_j, j = 1, \ldots, G-1.$$

Proof: If A commutes with the elements of $\mathbf{D}_N$, then it is circulant and satisfies $A^T = A$. The result follows immediately. □

Example: Consider the case, $N = 9, k = 3$, so that $G = 3$. If we first assume that the network has only $\mathbf{Z}_9$ symmetry, then Theorem 3.1 implies that

$$M^{-1}V \cap \mathbb{N}^9 = \{(\beta_0, \alpha_1, \alpha_2, \alpha_0, \alpha_1, \alpha_2, \alpha_0, \alpha_1, \alpha_2)^T, \text{ where } \beta_0, \alpha_0, \alpha_1, \alpha_2 \in \mathbb{N}\}. \tag{3.17}$$

Therefore $a_0 = \beta_0$, $a_1 = a_4 = a_7 = \alpha_1$, $a_2 = a_5 = a_8 = \alpha_2$, and $a_3, a_6 = \alpha_0$. If we also impose $\mathbf{D}_9$ symmetry, then

$$M^{-1}V \cap \mathbb{N}^9 = \{(\beta_0, \alpha_1, \alpha_1, \alpha_0, \alpha_1, \alpha_1, \alpha_0, \alpha_1, \alpha_1)^T, \text{ where } \beta_0, \alpha_0, \alpha_1 \in \mathbb{N}\}. \tag{3.18}$$

To satisfy (3.18) nontrivially, we can let $a_3 = a_6 = 1$, and set the rest of the coefficients in A to 0. This will lead to the coloring shown in Fig. 5A. A closer inspection of this solution shows that this network is not connected, and consists of three smaller subnetworks of three cells, as shown in Fig. 4. The other nontrivial balanced coloring that satisfies (3.18) comes from the complementary network $a_1 = a_4 = a_7 = 1$ and $a_2 = a_5 = a_8 = 1$, with $a_0 = a_3 = a_6 = 0$; see Fig. 5B. The only other option that satisfies (3.18) is an all-to-all coupled network. There are several options that satisfy (3.17) but not (3.18), corresponding to $\mathbf{Z}_N$ but not $\mathbf{D}_N$ symmetry. An example appears in Fig. 5C.

3.3 Connected Networks

As shown in both preceding examples, certain solutions to the given problem are trivial, since they result in networks that contain disconnected components. A network will be connected if and only if its connectivity matrix A is irreducible. Since $A \geq 0$ (that is, all of its elements are nonnegative), the irreducibility of A is equivalent to the positivity of $(I + A)^{N-1}$, where I is the $N \times N$ identity matrix [19], a condition which can be checked directly.

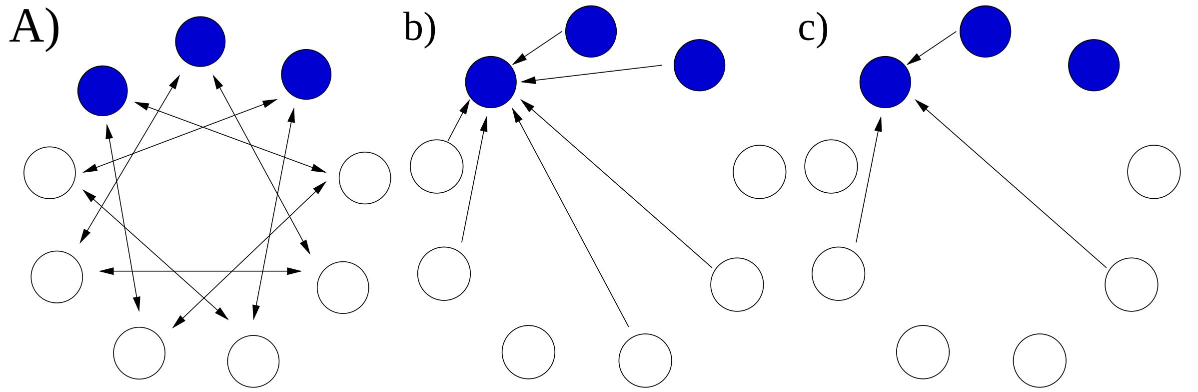

Figure 5: Three balanced colorings of 2 clusters in a network of nine cells. In A), $a_3 = a_6 = 1$ and $a_i = 0$ for all other i, such that each blue cell receives 2 white inputs and each white cell receives 1 blue input and 1 white input. Interchanging these values (but keeping $a_0 = 0$, corresponding to the absence of self-coupling) yields the architecture in B), where each cell gets inputs from 4 white cells and 2 blue cells. Both of these have $\mathbf{D}_N$ symmetry, while the architecture in C) ($a_1 = a_4 = a_7 = 1$ and $a_i = 0$ for all other i, such that each cell gets inputs from 2 white cells and 1 blue cell) has only $\mathbf{Z}_N$ symmetry. Note that in B) and C), connections analogous to those shown are repeated for all cells.

It is also useful to think of the directed graph (*digraph*) associated with the network, formed by taking each cell as a node and each connection as an edge. Because we consider coupling architectures with $\mathbf{Z}_N$ symmetry, the digraph obtained this way is *regular*, meaning that each node has the same number of incoming edges as all other nodes; indeed, this corresponds precisely to the fact that the connection matrix A is circulant. Since A is circulant, one of its eigenvalues is given by $\lambda^* = \sum_{j=0}^{N-1} a_{ij} = \beta_0 + (N/G-1)\alpha_0 + (N/G)(\alpha_1 + \ldots + \alpha_{G-1})$ [6]. A well-known result from graph theory states that the number of connected components in the digraph associated with A is exactly the algebraic multiplicity $am(\lambda^*)$ of the eigenvalue λ^* [5]. Thus, our network is connected if and only if $am(\lambda^*) = 1$.

An alternative derivation of a necessary and sufficient criterion for connectedness comes from a direct consideration of the network. Recall that in the labeling system we have used, within connectivity matrix A, the element $a_{0,j}, j = 0, \ldots, N-1$, denotes the number of connections to cell 0 from the cell j places away from it in the ring in an arbitrarily selected but fixed direction. Similar interpretations hold for $a_{i,j}, i \neq 0$, but we focus on $i = 0$ since we have assumed $\mathbf{Z}_N$ symmetry and A is thus circulant. By this $\mathbf{Z}_N$ symmetry, the network is connected if there exists $j \in \{0, \ldots, N-1\}$ such that j is relatively prime to N and $a_{0,j} \neq 0$. This follows immediately from the fact that if j, N are relatively prime, then the least common multiple of j and N is jN. In terms of the graph of the network, when such j exists, if we start at cell 0 and follow connections of length j in the specified direction, we will reach every other cell in the network before returning to cell 0. One special case is $\alpha_1 \neq 0$, corresponding to nearest neighbor coupling, which always fully connects the network, since $j = 1$ is relatively prime to every N.

The above criterion is not necessary; for example, in a network of $N = 12$ cells, full connectivity is achieved if $\alpha_0 = 0 = \alpha_1$ and $\alpha_2 \neq 0 \neq \alpha_3$, although neither 2 nor 3 is relatively prime to 12. However, this criterion generalizes to the following necessary and sufficient condition for connectedness:

Proposition 3.7 *Assume that a network of N cells has coupling matrix given by $A = circ(a_0, a_1, \ldots, a_{N-1})$ and consider a multisynchronous state with clusters of sizes $k, N-k$, such that $G = gcd(k, N) \neq 1$. For $j = 1, \ldots, N-1$, let $\gamma_j = j$ if $a_j \neq 0$ and let $\gamma_j = 0$ if $a_j = 0$. The network is connected if and only if there exist nonnegative integer coefficients $n_1, \ldots, n_{N-1}$ such that*

$$\sum_{i=1}^{N-1} n_i \gamma_i \equiv 1 \, (\mod N) \, . \tag{3.19}$$

Proof: First, consider whether there exists a path in the network from cell 1 to cell 0. Let $J = \{j \in 1, \ldots, N-1 : a_j \neq 0\}$. Note that if a path from cell 1 to cell 0 exists, then it consists of a sequence of connections of lengths that appear in J. If we choose n_j as the number of times that a connection of length j appears in this path, for each $j \in J$, then this choice yields a solution of equation (3.19), with n_j chosen arbitrarily for those j not in J.

Similarly, suppose that equation (3.19) has a solution $(n_1, \ldots, n_{N-1})$. In this case, starting from cell 1 and following n_j paths of length j, for each $j \in J$, yields a path from cell 1 to cell 0 composed of connections that do appear in the network architecture.

In summary, equation (3.19) has a solution $(n_1, \ldots, n_{N-1})$ if and only if there exists a path in the network from cell 1 to cell 0. Thus, when the network is connected, equation (3.19) has a solution, and when equation (3.19) has a solution, applying the network's $\mathbf{Z}_N$ symmetry yields a path from every other cell in the network to cell 0, such that the network is connected.

□

Remark 3.8 *Note that with $\mathbf{Z}_N$ symmetry, such that A is given by (3.11), the γ_j above are interrelated. In such a case, Proposition 3.7 can of course be rewritten using the elements α_j to define the terms γ_j. It does not, however, suffice to consider only $\gamma_1, \ldots, \gamma_{G-1}$. For example, if $N = 12$ and $G = 3$, then 2 divides N, but $a_{0,5} = a_{0,2} = \alpha_2$, so the condition $\alpha_2 \neq 0$ is enough to ensure that equation (3.19) can be satisfied. That is, even though $2n \not\equiv 1 \, (\mod 12)$ for each nonnegative integer n, we have $5n \equiv 1 \, (\mod 12)$ for an appropriate choice of n, such as $n = 5$.*

Finally, we note that while we consider disconnected architectures to be trivial, finding one is still useful, as the following proposition specifies.

Proposition 3.9 *If a pattern of synchrony is supported by a disconnected, but not completely uncoupled, architecture, then there exists a nontrivial connected architecture that supports it as well.*

Proof: For any choice of $\{\beta_0, \alpha_0, \alpha_1, \ldots, \alpha_{G-1}\}$ that satisfy equation (3.11), all complementary architectures, attained by making all nonzero elements zero and vice versa, also satisfy (3.11). Since the network has $\mathbf{Z}_N$ symmetry, it is easy to see that the complement of a disconnected network is connected. In particular, if a network is disconnected, then $a_{0,N-1} = 0 = a_{i,i+1}$ for $i = 0, \ldots, N-2$. It follows that in the complementary network, $a_{0,N-1} = a_{i,i+1} = 1$, and since nearest neighbors are coupled, the network must be connected. Similarly, choosing any nonzero values for $a_{0,N-1}$ and $a_{i,i+1}$ yields a connected network. These connected networks will be nontrivial (i.e., not coupled all-to-all) as long as the original network is not fully uncoupled.

□

Remark 3.10 *In fact, the complement of a disconnected network is connected in arbitrary networks, without the assumption of* $\mathbf{Z}_N$ *symmetry, by an analogous argument.*

4 Rings of cells of two types

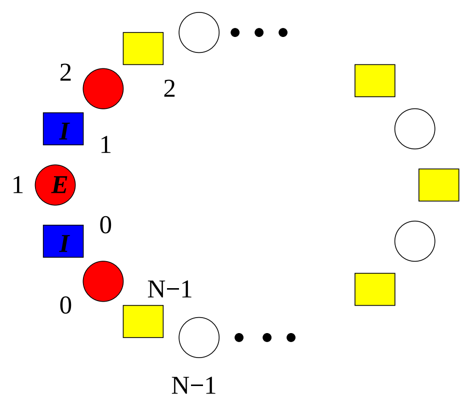

Figure 6: A ring network with two cell types, E and I. Cells of each type are numbered from 0 up to $N-1$, increasing in the clockwise direction, and each cell population is subdivided into two clusters, as shown.

We next develop a general theory for synchrony in rings of cells of two types. As an example, consider the network in Figure 6. There are two alternating types of cells in this ring; we can think of the round cells as E cells, and the rectangular cells as I cells. The cells are further subdivided into four synchronous groups. We will refer to this architecture as a *double ring*. As discussed previously, all cells in a synchronous group will be referred to as having the same color. Our goal is to describe the architectures that will support an activity pattern in which groups of k and $N-k$ adjacent E cells and l and $N-l$ adjacent I cells, as shown in Fig. 6, evolve synchronously. Note that the two clusters of E cells and the I cells need themselves not be adjacent, although they are shown as being adjacent in Fig. 6.

In general, we cannot expect cells to be exactly synchronous unless they are of the same type. Two E or I cells can be expected to be synchronous only if their input sets are identical [23, 13]. This situation is a direct generalization of the one one described in section 2.2, with the exception that there are two input sets $\mathcal{C}_i^E$ and $\mathcal{C}_i^I$ into each cell, corresponding to the two types of cells in the networks. Two cells of the same type can exhibit robust synchrony only when there are bijections $\phi^E : \mathcal{C}_i^E \to \mathcal{C}_j^E$ and $\phi^I : \mathcal{C}_i^I \to \mathcal{C}_j^I$ that carry the inputs to cell i from each synchronous group to inputs to cell j from the same group. member of a synchronous group to those of another group member.

Denote the connectivity matrices between the E cells and the I cells by A^{EE} and A^{II}, respectively (these matrices connect cells of equal type). In addition, the matrices A^{EI} and A^{IE} will represent connections from I to E cells and from E to I cells, respectively. As in the previous section, if we assume that the network has $\mathbf{Z}_N$ symmetry, then all of these matrices are circulant. For example, $A^{EE} = \text{circ}\,(a_0^{EE}, a_1^{EE}, \ldots, a_{N-1}^{EE})$, since there are N E cells. The cells in the network are numbered by assigning the first cell in the group of k synchronous E cells the number 0, and proceeding clockwise. The I cells are numbered similarly (see Fig. 6).

Let R^0, R^1, R^2 and R^3 be 4-vectors that denote the total number of inputs to each of the different cell types, where the labels 0,1,2, and 3 denote red and white E cells, and blue and yellow I cells respectively. For instance, R_1^0 is the total number of inputs to the red E cells from the white E cells. Similarly, let $e_0 = \ldots = e_{k-1} = (1, 0, 0, 0)^T$, $e_k = \ldots = e_{N-1} = (0, 1, 0, 0)^T$, and $d_0 = \ldots = d_{l-1} = (0, 0, 1, 0)^T$, $d_l = \ldots = d_{N-1} = (0, 0, 0, 1)^T$ denote the cells in the two different groups, as in the previous section.

The condition that the input sets of two E cells sharing the same color are equivalent leads to the following set of equations

$$
\begin{aligned}
a_0^{EE} e_0 + \ldots + a_{N-1}^{EE} e_{N-1} + a_0^{EI} i_0 + \ldots + a_{N-1}^{EI} i_{N-1} &= R^0 \\
a_{N-1}^{EE} e_0 + \ldots + a_{N-2}^{EE} e_{N-1} + a_{N-1}^{EI} i_0 + \ldots + a_{N-2}^{EI} i_{N-1} &= R^0 \\
\ldots & \\
a_1^{EE} e_0 + \ldots + a_0^{EE} e_{N-1} + a_1^{EI} i_0 + \ldots + a_0^{EI} i_{N-1} &= R^1,
\end{aligned}
\tag{4.20}
$$

where R^0 appears on the right hand side in the first k equations and R^1 appears on the right hand side in the next $N-k$ equations. A similar set of equations, involving the matrices A^{IE} and A^{II}, holds for the I cells.

This set of equations (4.20) splits into two independent groups. Note that for the matrices A^{EE} and A^{II} we obtain equations that are equivalent to (3.7). This observation follows directly from the way the problem is set up: the E to E and I to I connections that support a given pattern of synchrony are determined independently of the other connections in the network. Therefore Theorem 3.1 can be used directly to determine the structure of these matrices.

For the connections from the I to the E cells, we obtain from equation (4.20) the equations

$$
\begin{array}{rlrl}
a_0^{EI} + a_1^{EI} + \ldots + a_{l-1}^{EI} &= R_2^0 & a_l^{EI} + \ldots + a_{N-1}^{EI} &= R_3^0 \\
& \ldots\ldots & & \\
a_{N-k+1}^{EI} + a_{N-k+2}^{EI} + \ldots + a_{N-k+l}^{EI} &= R_2^0 & a_{N-k+l+1}^{EI} + \ldots + a_{N-k}^{EI} &= R_3^0 \\
a_{N-k}^{EI} + a_{N-k+1}^{EI} + \ldots + a_{N-k+l-1}^{EI} &= R_2^1 & a_{N-k+l}^{EI} + \ldots + a_{N-k-1}^{EI} &= R_3^1 \\
& \ldots\ldots & & \\
a_1^{EI} + a_2^{EI} + \ldots + a_l^{EI} &= R_2^1 & a_{l+1}^{EI} + \ldots + a_0^{EI} &= R_3^1
\end{array}
\tag{4.21}
$$

As in the case of equation (3.7), the left and right columns are equivalent. As in section 3.1 , we reorder the equations from the left column and put the first equation first, and then follow with the last equation up to the second equation. Once reordered, we have

$$
Ma^{EI} = R \tag{4.22}
$$

where

$$
a^{EI} = (a_0^{EI}, a_1^{EI}, \ldots, a_{N-1}^{EI})^T \tag{4.23}
$$

$$
R = (R_2^0, \underbrace{R_2^1, \ldots, R_2^1}_{N-k \text{ times}}, R_2^0, \ldots, R_2^0)^T \tag{4.24}
$$

and

$$
M = \begin{bmatrix}
1 & 1 & 1 & \ldots & 1 & 0 & 0 & \ldots & 0 & 0 \\
0 & 1 & 1 & \ldots & 1 & 1 & 0 & \ldots & 0 & 0 \\
0 & 0 & 1 & \ldots & 1 & 1 & 1 & \ldots & 0 & 0 \\
 & & & \ldots & & & & \ldots & & \\
1 & 1 & 1 & \ldots & 0 & 0 & 0 & \ldots & 0 & 1
\end{bmatrix} \tag{4.25}
$$

where each row contains $N - l$ zero entries. We obtain the same equation for the matrix A^{IE}, with the roles of k and l reversed.

The problem of solving equation (4.22) is virtually identical to solving equation (3.8) with (3.9). The difference, which somewhat complicates the calculations, is that in the present case k does not necessarily equal l.

Theorem 4.1 *Suppose that a network composed of N E cells and N I cells forms a double ring, and that groups of k and $N-k$ adjacent E cells and l and $N-l$ adjacent I cells form synchronous clusters. Let $G_k = gcd(k, N)$ and $G_l = gcd(l, N)$. The connectivity matrices that can support this form of synchrony between identical cells are given by*

$$
A^{EE} = \ circ\ (\beta_0^{EE}, \alpha_1^{EE}, \ldots, \alpha_{G_k-1}^{EE}, \alpha_0^{EE}, \alpha_1^{EE}, \ldots \alpha_{G_k-1}^{EE}, \alpha_0^{EE}, \ldots, \ldots, \alpha_{G_k-1}^{EE}),
$$

$$
A^{II} = \ circ\ (\beta_0^{II}, \alpha_1^{II}, \ldots, \alpha_{G_l-1}^{II}, \alpha_0^{II}, \alpha_1^{II}, \ldots \alpha_{G_l-1}^{II}, \alpha_0^{II}, \ldots, \ldots, \alpha_{G_l-1}^{II}),
$$

where all entries are in $\mathbf{N} \cup \{0\}$.

The connectivity matrix A^{EI} has the form

$$A^{EI} = \text{ circ } (\beta_0^{EI}, \alpha_1^{EI}, \ldots, \alpha_{G_l-1}^{EI}, \beta_{G_l}^{EI}, \alpha_1^{EI}, \ldots \alpha_{G_l-1}^{EI}, \beta_{2G_l}^{EI}, \ldots, \beta_{N-G_l}^{EI}, \alpha_1^{EI}, \ldots, \alpha_{G_l-1}^{EI}).$$

If $k \equiv 0$ (mod G_l), then the coefficients $\beta_0, \beta_l, \beta_{2l}, \ldots$ split into two equivalence classes

$$\begin{aligned} \beta_l = \beta_{2l} = \ldots = \beta_{N-k} \\ \beta_{N-k+l} = \beta_{N-k+2l} = \ldots = \beta_0 \end{aligned} \tag{4.26}$$

where all subscripts are taken modulo N. If $k \not\equiv 0$ (mod G_l), then there is only one equivalence class

$$\beta_l = \beta_{2l} = \ldots = \beta_0.$$

The same holds for A^{IE} with the roles of k and l reversed.

Remark 4.2 *If $k = l$, so that the two clusters contain the same number of cells, then, since $N - k + l = N$, the sets of matrix entries in (4.26) are composed of β_0 in one class, and the remaining entries in the second. The matrix A^{EI} has therefore the same form as A^{EE} and A^{II} in this case. However, note that the coefficient $a_0^{EI} = \beta_0^{EI}$ gives the number of connections from the j-th I cell to the j-th E cell, while a_0^{EE} and a_0^{II} give the number of self couplings of each E and I cell, respectively.*

Proof: We need to find solutions to four problems of the form

$$Ma \in V \tag{4.27}$$

where

$$V = Rw_1 \oplus Sw_2 \stackrel{\text{def}}{=} R(1, 1, 1, \ldots, 1)^T \oplus S(1, 0, 0, \ldots, 0, 1, 1, \ldots, 1)^T.$$

The number of zeroes in a row of M, and in w_2, both equal to $N - k$ and $N - l$ in the cases of A^{EE} and A^{II}, respectively, and therefore Theorem 3.1 can be applied directly.

In the case of A^{EI}, the matrix M has $N - l$ zero entries, while w_2 has $N - k$ zero entries. Since w_1 and M have the same form as in section 3.1, we can proceed as in the proof of Theorem 3.1 to find $C\tilde{M}^{-1}C^{-1}(\mathbf{C}w_1)$ and obtain the same result as in (3.16).

A similar argument can be used to obtain $C\tilde{M}^{-1}C^{-1}(\mathbf{C}w_2)$, although the calculations are lengthy. Rather than providing these calculations we provide a short proof, which uses the $\mathbf{Z}_N$ symmetry of the system directly.

We will use the structure of the left column in equations (4.21), which determine all possible values for a^{EI}. Suppose that the right hand sides of two adjacent equations are equal. Then subtracting the two equations leads to $a_j^{EI} = a_{j-l}^{EI}$ for some j, where the indices are taken modulo N. We therefore obtain all equations of the form $a_j^{EI} = a_{j-l}^{EI}$, except for two. The two missing equations are

$$a_0^{EI} = a_l^{EI} \qquad \text{and} \qquad a_{N-k}^{EI} = a_{N-k+l}^{EI}. \tag{4.28}$$

If these equalities were included with the remaining $N-2$ equalities, the coefficients a_j^{EI} would form $G_l = gcd(l, N)$ equivalence classes. Each set of equalities defining an equivalence class would form a "ring", in the sense that

$$a_j^{EI} = a_{j+l}^{EI} = \ldots = a_{j+\frac{lN}{G_l}}^{EI} = a_j^{EI}. \tag{4.29}$$

Therefore, it is necessary to remove more than one equality defining this equivalence class to split it into two classes. That is, the coefficients $\beta_0, \beta_l, \beta_{2l}, \ldots$ split into two classes, as described in (4.26), if and only if the equalities in (4.28) both come from the same "ring" of equations defined by (4.29).

Since N and l are both multiples of G_l, it can now be easily checked that if $k \not\equiv 0$ (mod G_l), then the equality $a_{N-k}^{EI} = a_{N-k+l}^{EI}$ is not in the set of equalities defining the equivalence class of a_0^{EI}, and there are G_l equivalence classes for the coefficients. On the other hand, if $k \equiv 0$ (mod G_l), then removing the two equalities (4.28) breaks the equivalence class of a_0^{EI} into two in the way described in (4.26). □

From the proof of Theorem 4.1, it is clear that Theorem 4.1 holds regardless of where the l I cells are positioned relative to the k E cells; adjacency of the clusters is not needed. The lengths of the connections corresponding to the elements of the connection matrix depend on these positions, however, so application of the Theorem implies that different relative cluster positions will be supported by different coupling architectures.

Example: Consider again the example of $N = 7$ discussed in section 2.3. In the case of a double ring of 7 E cells and 7 I cells, $G_k = G_l = 1$ for any choice of k, l. Thus, A^{EI} is a 7 by 7 matrix of the form $A^{EI} = circ(\beta_0^{EI}, \beta_1^{EI}, \ldots, \beta_6^{EI})$. Suppose, for example, that $k = 3$, as in Fig. 1, such that $k \equiv 0 \, (\text{mod} \, G_l)$ and equations (4.26) apply. If $l = 2$, then equations (4.26) yield

$$\beta_2 = \beta_4; \beta_6 = \beta_1 = \beta_3 = \beta_5 = \beta_0. \tag{4.30}$$

Equation (4.30) gives rise to two nontrivial (and complementary) architectures of I to E connections, each corresponding to setting the elements of one of the equivalence classes of connections equal to 1 and setting the other class equal to 0. These are displayed in Fig. 7A,B; the second of these also appears in Fig. 1. Interestingly, if $l = N - 2 = 5$, then we get different equivalence classes, namely

$$\beta_5 = \beta_3 = \beta_1 = \beta_6 = \beta_4; \beta_2 = \beta_0. \tag{4.31}$$

The two corresponding nontrivial architectures of I to E connections derived from (4.31) are shown in Fig. 7C,D.

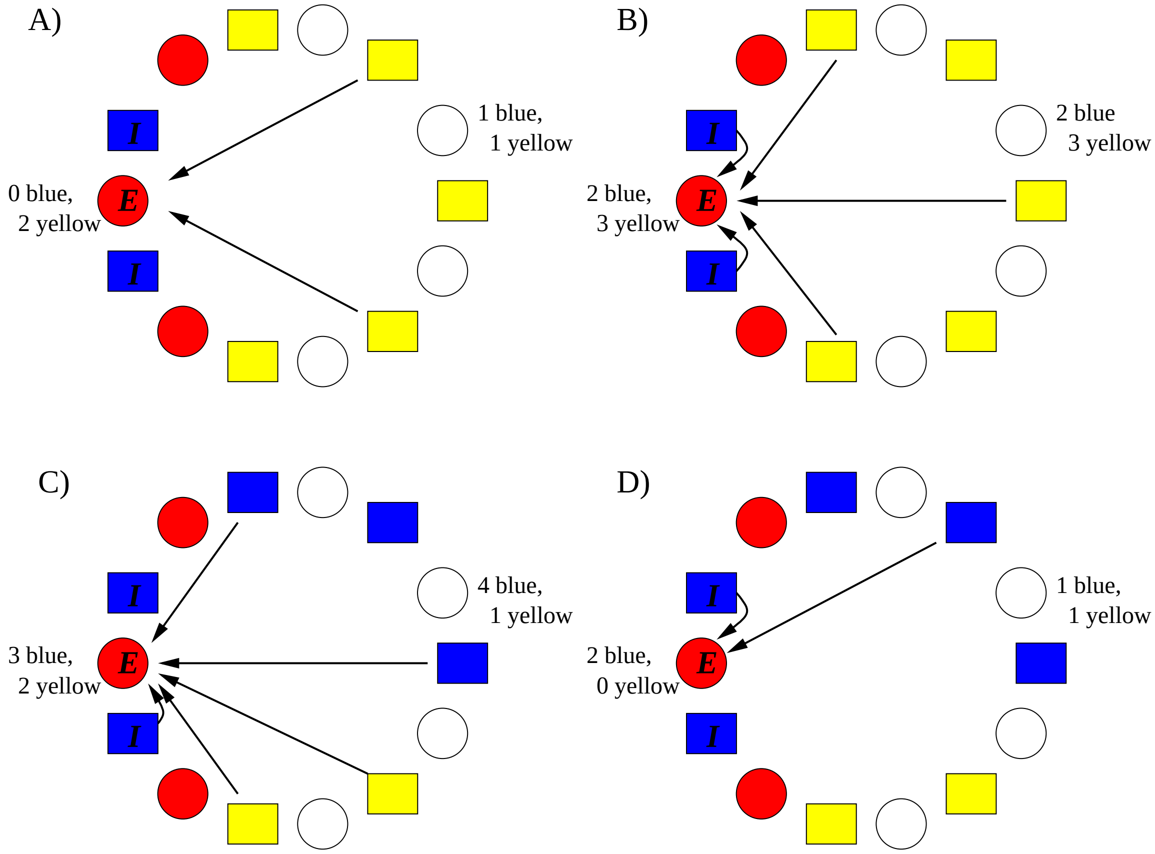

Figure 7: Architectures of I to E connections yielding balanced colorings in a ring of 7 E cells and 7 I cells, grouped in 4 clusters. In each figure, we only show the connections to a particular E cell, but each E cell receives an analogous pattern of inputs as dictated by $\mathbf{Z}_N$ symmetry. The text indicates the number of each connection type received by each E cell in each cluster (all E cells of the same color receive the same number of each connection type since these are balanced colorings). The top figures correspond to the equivalence classes, for $l = 2$, given in equation (4.30), with $\beta_2 = \beta_4 = 1, \beta_6 = \beta_1 = \beta_3 = \beta_5 = \beta_0 = 0$ in A) and $\beta_2 = \beta_4 = 0, \beta_6 = \beta_1 = \beta_3 = \beta_5 = \beta_0 = 1$ in B). The bottom figures correspond to the equivalence classes, for $l = 5$, given in equation (4.31), with $\beta_5 = \beta_3 = \beta_1 = \beta_6 = \beta_4 = 1, \beta_2 = \beta_0 = 0$ in C) and $\beta_5 = \beta_3 = \beta_1 = \beta_6 = \beta_4 = 0, \beta_2 = \beta_0 = 1$ in D).

The case of $l = 5$ leads to different architectures than those arising in the case of $l = 2$, even though $5 = 7 - 2$, because the results of Theorem 4.1 are derived by assuming that the clusters of k E cells and l I cells are aligned as shown in Fig. 6. As noted earlier, analogous results to Theorem 4.1 can be derived for other relative positions of these clusters, using the same methods. As one of the clusters is moved around the ring, the numbering changes, and, although one obtains the same solution in terms of coupling matrix coefficients, the architectures will look different.

Of course, by switching the labels on the cells in this example, we can attain a balanced coloring with a nontrivial coupling architecture for mutlisynchronous states with E cell clusters of sizes 2 and 5 and I cell clusters of sizes 3 and 4. As noted earlier, E cell clusters of sizes 3 and 4, or of sizes 2 and 5, would only be possible with trivial coupling architectures in a single ring of 7 E cells, by Corollary 3.3.

5 Discussion

Coupling architecture is frequently crucial in determining the dynamical behavior of a coupled network. To model a collection of interacting cells, it is therefore necessary to have accurate information about the ways in which the cells interact. Unfortunately, in areas such as experimental neuroscience, such information may be very difficult to obtain directly.

The method we presented provides a means of determining possible network architectures based on observed activity patterns. The architectures obtained using this analysis are the only ones within their class that can support the given activity patterns robustly, without the presence of specialized features in the intrinsic dynamics of the cells in the network. This information could be useful in selecting coupling architectures to use in models of networks known to produce certain activity patterns, in designing novel networks to produce particular activity patterns, or in deducing the actual architectural properties of physical networks.

Without imposing certain constraints, the architectural constraint problem becomes too general. It is important to restrict to a general class of architectures to start the process, in order to narrow the number of possibilities and eliminate trivialities. In the examples considered, this restriction was given by the requirement that the network have $\mathbf{Z}_N$ or $\mathbf{D}_N$ symmetry.

Although we did not discuss the stability of the invariant subspaces corresponding to the different multisynchronous states, in certain examples the techniques developed in [1, 2] will be applicable. The invariant subspaces corresponding to different multisynchronous patterns can be nested, exactly as in in the case in which the multisynchronous states in a network are determined by symmetry [4, 1, 2]. The network architecture determines the invariant subspaces and how they are nested. In this situation, synchrony breaking bifurcations can occur as a multisynchronous solution bifurcates to another contained in an invariant subspace of higher dimension (a simple example is the transition from a fully synchronous, i.e. one color solution to a two color solution). Such transitions correspond to symmetry breaking bifurcations in equivariant bifurcation theory, although in the present case neither the bifurcating nor the resulting solutions need to be symmetric.

Rings of interacting cells are frequently used as models of neuronal systems; however, the method we present can be generalized in many ways. The description of multisynchronous states, given in Section 2.2, is valid even in nonsymmetric networks. The approach given in the proof of Theorem 3.1 can be generalized to any network whose symmetries are given by an abelian group. We believe that a similar approach is valid more generally, although current representation theory would have to be extended to deal with such cases.

It was shown in Section 4 that the method can be extended to networks with multiple types of cells. One result of this extension is that coupling a particular network of cells to cells of a second type can greatly expand the range of architectures that can balance a particular coloring of the original cells. If a network of one cell type has N cells with $gcd(k, N) = 1$, then a 2-cluster state with clusters of sizes k and $N - k$ will be balanced if and only if the network is uncoupled or all-to-all coupled; however, synchrony is never stable in uncoupled systems. Our results show that under fairly general conditions (see Theorem 4.1), if N cells of a second type are interleaved with the original cells, then a balanced coloring featuring the same two clusters in the original cells can be achieved by leaving the original cells uncoupled but coupling the cell types together in a non-trivial way. Such coupling across types can infer stability on synchronized states (e.g. [26, 22, 21, 18]). More generally, the possibility of connections between two cell types tends to allow for a greater variety of architectures that support particular multisynchronous states. In addition to multiple cell types, similar ideas to those presented here can be used to treat networks with multiple arrow types (in which identical cells may not interact in identical ways) and multiple connections between cells.

In all of the solutions considered, cells in the same cluster are assumed to be adjacent to each other in the ring. In a particular system, this adjacency need not correspond to actual physical proximity. In the mammalian visual cortex, for example, a natural ring structure can be defined in terms of cells' orientation preferences, rather than their spatial positions. Our results apply as long as, once the cells are ordered according to some criterion, the coupling architecture features $\mathbf{Z}_N$ symmetry. Nonetheless, it would be of interest to extend our results to clustered solutions with non-adjacent elements, such as traveling waves on a ring, in which cells a certain wavelength apart in the ring activate together, followed by their neighbors to one side, and so on, until the pattern repeats.

Acknowledgments. This work was supported in part by NSF grants DMS-0244529 (KJ) and DMS-0108857 (JR). We thank Martin Golubitsky for helping to get this work started and for many helpful discussions and comments. JR also thanks E. Glen Whitehead for suggestions on some useful references in algebraic graph theory.

References

[1] V. Belykh, I. Belykh, and M. Hasler. Hierarchy and stability of partially synchronous oscillations of diffusively coupled dynamical systems. *Phys. Rev. E*, 62(5):6332–6345, 2000.

[2] V. N. Belykh, I. V. Belykh, and E. Mosekilde. Cluster synchronization modes in an ensemble of coupled chaotic oscillators. *Phy. Rev. E*, 63:036216–1–4, 2001.

[3] H. Bergman, A. Feingold, A. Nini, A. Raz, H. Slovin, M. Abeles, and E. Vaadia. Physiological aspects of information processing in the basal ganglia of normal and parkinsonian primates. *Trends Neurosci.*, **21**:32–38, 1998.

[4] P. C. Bressloff and S. Coombes. Symmetry and phase-locking in a ring of pulse-coupled oscillators with distributed delays. *Phys. D*, 126(1-2):99–122, 1999.

[5] D. Cvetković, M. Doob, and H. Sachs. *Spectra of Graphs: Theory and Applications*. Academic Press, New York, 1979.

[6] P. Davis. *Circulant Matrices*. John Wiley & Sons, New York, 1979.

[7] A. Destexhe, D. Contreras, and M. Steriade. Mechanisms underlying the synchronizing action of corticothalamic feedback through inhibition of thalamic relay cells. *J. Neurophys.*, **79**:999–1016, 1998.

[8] A. Destexhe and T. Sejnowski. Synchronized oscillations in thalamic networks: insights from modeling studies. In M. Steriade, E. Jones, and D. McCormick, editors, *Thalamus, Volume II*, pages 331–372. Elsevier, Amsterdam, 1997.

[9] A. Engel, P. Fries, and W. Singer. Dynamic predictions: oscillations and synchrony in top-down processing. *Nat. Rev. Neurosci.*, **2**:704–716, 2001.

[10] M. Golubitsky, M. Nicol, and I. Stewart. Some curious phenomena in coupled cell systems. *J. Nonlinear Sci*, **14**:119–136, 2004.

[11] M. Golubitsky, I. Stewart, P. Buono, and J. Collins. A modular network for legged locomotion. *Physica D*, **115**:56–72, 1998.

[12] M. Golubitsky, I. Stewart, P. Buono, and J. Collins. Symmetry in locomotor central pattern generators and animal gaits. *Nature*, **401**:693–695, 1999.

[13] M. Golubitsky, I. Stewart, and A. Torok. Patterns of synchrony in coupled cell networks with multiple arrows. Submitted.

[14] J. Hoover and P. Strick. The organization of cerebellar and basal ganglia outputs to primary motor cortex as revealed by retrograde transneuronal transport of herpes simplex virus type 1. *J. Neurosci.*, **19**:1446–1463, 1999.

[15] J. Hopfield and C. Brody. What is a moment? "Cortical" sensory integration over a brief interval. *Proc. Natl. Acad. Sci. (USA)*, **97**:13919–13924, 2000.

[16] J. Hopfield and C. Brody. What is a moment? Transient synchrony as a collective mechanism for spatiotemporal integration. *Proc. Natl. Acad. Sci. (USA)*, **98**:1282–1287, 2001.

[17] N. Kopell, G. Ermentrout, M. Whittington, and R. Traub. Gamma rhythms and beta rhythms have different synchronization properties. *Proc. Natl. Acad. Sci. (USA)*, **97**:1867–1872, 2000.

[18] S. Kunec and A. Bose. High-frequency, depressing inhibition facilitates synchronization in globally inhibitory networks. *Network: Comp. Neural. Sys.*, **14**:647–672, 2003.

[19] H. Minc. *Nonnegative Matrices*. John Wiley & Sons, New York, 1988.

[20] A. Pikovsky, M. Rosenblum, and J. Kurths. *Synchronization: A Universal Concept in Nonlinear Science*. Cambridge University Press, Cambridge, 2003.

[21] J. Rubin and D. Terman. Analysis of clustered firing patterns in synaptically coupled networks of oscillators. *J. Math. Biol.*, **41**:513–545, 2000.

[22] J. Rubin and D. Terman. Geometric analysis of population rhythms in synaptically coupled neuronal networks. *Neural Comput.*, **12**:597–645, 2000.

[23] I. Stewart, M. Golubitsky, and M. Pivato. Symmetry groupoids and patterns of synchrony in coupled cell networks. *SIAM J. Appl. Dynam. Sys.*, 2:609–646, 2003.

[24] S. Strogatz. *Sync: The Emerging Science of Spontaneous Order*. Hyperion, New York, 2003.

[25] D. Terman, J. Rubin, A. Yew, and C. Wilson. Activity patterns in a model for the subthalamopallidal network of the basal ganglia. *J. Neurosci.*, **22**:2963–2976, 2002.

[26] D. Terman and D. L. Wang. Global competition and local cooperation in a network of neural oscillators. *Physica D*, **81**:148–176, 1995.